Nanotechnology Coatings for Erosion Protection of Turbine Components

V. P. "Swami" Swaminathan
TurboMet International,
San Antonio, TX 78250

Ronghua Wei
Southwest Research Institute,
San Antonio, TX 78238

David W. Gandy
Electric Power Research Institute,
Charlotte, NC 28262

Solid particle erosion (SPE) and liquid droplet erosion (LDE) cause severe damage to turbine components and lead to premature failures, business loss, and repair costs to power plant owners and operators. Under a program funded by the Electric Power Research Institute, TurboMet International and Southwest Research Institute (SRI) have developed hard erosion resistant nanocoatings and have conducted evaluation tests. These coatings are targeted for application in steam and gas turbines to mitigate the adverse effects of SPE and LDE on rotating blades and stationary vanes. Based on a thorough study of the available information, the most promising coatings, such as nanostructured titanium silicon carbonitride (TiSiCN), titanium nitride (TiN), and multilayered nanocoatings, were selected. State-of-the-art nanotechnology coating facilities at SwRI were used to develop the coatings. The plasma enhanced magnetron sputtering method was used to apply these coatings on various substrates. Ti–6Al–4V, 12Cr, 17-4PH, and custom 450 stainless steel substrates were selected based on the current alloys used in gas turbine compressors and steam turbine blades and vanes. Coatings with up to 30 μm thickness have been deposited on small test coupons. Initial screening tests on coated coupons by solid particle erosion testing indicate that these coatings have excellent erosion resistance by a factor of 20 over the bare substrate. Properties of the coating, such as modulus, hardness, microstructural conditions including the interface, and bond strength, were determined. Tensile and high-cycle fatigue tests on coated and uncoated specimens indicate that the presence of the coatings has no negative effects but has a positive influence on the high-cycle fatigue strength at zero and high mean stresses.
[DOI: 10.1115/1.3028567]

Introduction

Solid particle erosion (SPE) and liquid droplet erosion (LDE) cause severe damage to turbine components such as gas turbine compressor blades and vanes; high-pressure steam turbine inlet stage and later stage low-pressure (LP) turbine blades. Some examples of such damage are shown in Fig. 1. SPE reduces turbine efficiency and reliability by eroding the airfoils and potentially leading to catastrophic failures during service. There were several turbine failures attributed to such damage in service. In the case of flight engines, it may endanger the lives of the crew and passengers especially for flight engines operated in dusty environments [1,2]. In addition to SPE, LDE in the steam path of steam turbines also leads to damage of the nozzles and blades [3]. For LM600 Sprint gas turbines using water injection, significant LDE damage was observed on the leading edge of compressor blades [4]. Similar damage to Frame FA engine R-0 compressor blades was reported and some of the field failures were attributed to such damage. Various coatings have been applied to combat erosion in turbines. The most commonly used are nitride coatings, including single layered TiN, ZrN, CrN, and TiAlN; multilayered Cr/CrN and Ti/TiN; and superlattice CrN/NbN. Conventional physical vapor deposition (PVD), modified electron beam physical vapor deposition (EB-PVD), and cathode arc physical vapor deposition (CAPVD) are the methods used to deposit these coatings. It is known that relatively thick coatings are needed for durable erosion resistance. Rickerby and Burnett [5] observed that thick TiN coatings on both stainless steel and carbon steel showed better erosion resistance than thin coatings.

In recent years, nanocomposite coatings (mainly nanocrystalline TiN in a matrix of amorphous Si_3N_4 or nanocomposite TiN/Si_3N_4) have been actively studied by a number of research groups worldwide using mostly chemical vapor deposition (CVD) and sometimes PVD (in particular, magnetron sputtering) [6–9] These coating are extremely hard and have shown great wear resistance in laboratories. For tribological applications, such as in machine tools, thin coatings of 2–5 μm are commonly used. However, in this project, nanocomposite coatings (10–30 μm thick) have been produced, and their erosion resistance was measured with good results.

Plasma enhanced magnetron sputter (PEMS) deposition is an improved version of conventional magnetron sputtering. It utilizes an electron source and a discharge power supply to generate plasma, independent of the magnetron plasma, in the entire vacuum chamber. The PEMS technology has been shown to produce much better TiN coatings for cutting applications [10,11], and the superior performance is attributed to the very fine grain (60 nm or less) TiN microstructure that is formed due to the heavy ion bombardment [12].

The objective of this Electric Power Research Institute (EPRI) project is to develop erosion resistant nanotechnology coatings using the PEMS method to mitigate the erosion problems encountered in gas and steam turbines under SPE and LDE conditions. The technical approach is as follows.

- Apply selected coatings by the plasma enhanced magnetron sputtering method on the substrate material used in the turbine blades and vanes.
- Conduct screening tests, such as SPE, LDE, hardness, adhesion ranking, etc., on small samples to identify the most promising coating(s). Corrosion tests are also planned but have not been initiated at the time of this paper.

Manuscript received May 17, 2008; final manuscript received September 10, 2008; published online May 18, 2010. Review conducted by Dilip R. Ballal. Paper presented at the ASME Turbo Expo 2008: Land, Sea and Air (GT2008), June 9–13, 2008, Berlin, Germany.

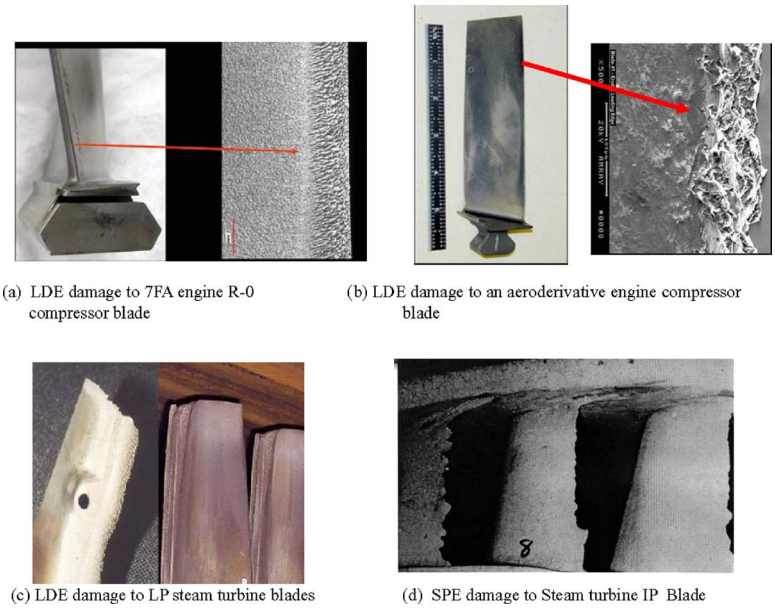

(a) LDE damage to 7FA engine R-0 compressor blade

(b) LDE damage to an aeroderivative engine compressor blade

(c) LDE damage to LP steam turbine blades

(d) SPE damage to Steam turbine IP Blade

Fig. 1 Examples of SPE and LDE damage to combustion and steam turbine components

- Compare the properties of these samples with similar results from other commercial techniques.
- Develop coating process specifications for the selected coatings.
- Conduct qualification testing by mechanical property evaluations and thermal exposure tests to simulate field service conditions.
- Apply coating(s) to components and conduct field evaluations.
- Commercialize the technology.

Three selected coatings were applied to small disk samples prepared from four substrate alloys. One of the important tasks is to identify the most effective combination of the processing variables to produce the best coating possible by the PEMS method. Several combinations of the processing variables have been tried initially on Ti–6Al–4V substrate samples to select the optimum combination. Screening tests have been completed on all of the selected coatings and the most promising coatings have been identified. Under Phase II of this project, three coatings have been applied to mechanical and thermal test specimens and tests are in progress to qualify the coatings prior to field application. Then the selected coatings will be applied to turbine components under Phase II for field service exposure and durability evaluations in operating turbines.

Results of the evaluations of some of the TiN and TiSiCN coatings produced under some of the deposition conditions were previously reported [13]. This paper summarizes the evaluation results on coatings produced with additional combinations of processing variables based on a statistical design of experiment approach to select the best combination of coating deposition parameters. Results from monolayer and multilayer coatings are presented.

Experimental Details

Substrate materials. Substrate alloys, Ti–6Al–4V alloy, 12Cr (Type 403), 17-4PH, and custom 450 stainless steels were selected for this study. These materials are used in gas turbine compressors and steam turbine blades and vanes. Some of the samples were directly machined from scrapped turbine blades and some were machined from rod stock. Test samples were machined to 2.5 cm (1 in.) in diameter by 3.2 mm (0.125 in.) thick and then polished using 1 μm diamond paste to a surface roughness of ~5 nm Ra. This fine surface finish was used in the initial development phase of the coatings. For this study some of the samples were also ground to 600 grit rougher surface finish, which is ~85 nm Ra. They were cleaned with acetone and methanol before entering the PEMS vacuum chamber for coating deposition.

Plasma enhanced magnetron sputtering process. Figure 2 shows a schematic of the PEMS system at Southwest Research Institute (SwRI). The PEMS technology utilizes magnetron-generated plasma and an additional electron source (a heated filament, for instance) and a discharge power supply to generate plasma. This electron-source generated plasma is independent of the magnetron-generated plasma. There are a number of advantages to this technique. First, during the substrate sputter-cleaning, the magnetrons are not operated, while the electron-source generated plasma alone is sufficient to clean the substrate. In this way, deposition of the target material, which is of concern for conventional magnetron sputtering, will not occur, and the cleaning of the sample surface is assured. Second, during the film deposition, the ion bombardment from the electron-source generated plasma is very intense and the current density at the sample surfaces can be 25 times higher than that with the magnetron-generated plasma alone. Consequently, a high ion-to-atom ratio can be achieved in the chamber. Improvement in the microstructure of the coating as a function of the ion bombardment intensity was observed [13]. The microstructure consists of hard nanocrystals of TiCN surrounded by amorphous SiCN. The nanocoatings in general have a grain size of less than 100 nm, which produces high hardness. X-ray diffraction analysis of the current coating shows a grain size the of 10 nm, a factor of 10 better than what is normally considered nanostructure coatings [13].

The nominal deposition procedures in this study included argon sputter-cleaning of the samples for 60–90 min to remove the residual oxide on the surface. Then the samples were coated with a "bond layer" of pure Ti metal for about 5 min, which corresponds to 200 nm for Ti. After that, deposition of the hard erosion resistant coating is started. In preparing the single-phased nitride of TiN, a solid target of Ti is used in a mixture of $Ar+N_2$ gases. A Stellite 6 alloy plate was used to deposit the stellite nanocoating. In preparing the nanocomposite coatings, trimethylsilane ($(CH_3)_3SiH$) or (TMS) gas was used as the precursor during sputtering of Ti to form $TiSi_xC_yN_z$ in the PEMS process. Traditionally,

(a) Schematic diagram (b) PEMS Chamber and control module (c) Plasma during coating

Fig. 2 Plasma enhanced magnetron sputtering system with two magnetrons

Ti–Si–C–N coating is prepared using CVD processes [14–17]. However, both $TiCl_4$ and $SiCl_4$ were used in these studies. Trimethylsilane is much easier and safer to handle and does not have any adverse effect on the vacuum chamber and pumps. Two circular magnetrons of 17.5 cm (6.9 in.) diameter were positioned on the opposite sides of the coating chamber in this process. Several processing variables were controlled, as described in Ref. [13].

The sample temperature was measured using a thermocouple embedded in the samples and the steady state temperature was typically about 400°C (752°F). At this temperature the base alloy properties are not expected to change. The various deposition parameters and thus, the deposition rates are carefully controlled to manage the substrate temperature during the coating process.

Characterization of Hard Coating. The following laboratory evaluation tests were conducted on the coated samples:

- nanoindentation to obtain the nanohardness and elastic modulus
- Rockwell C hardness indentations to qualitatively compare coating adhesion
- scratch testing for a quantitative assessment of the adhesion strength
- scanning electron microscopy (SEM) to examine the morphology and microstructure on the cross section
- solid particle erosion tests per ASTM Standard G76-04 using a nozzle at incident angles of 30 deg and 90 deg with respect to the sample surface
- LDE tests at 90 deg incident angle

Nanohardness was measured on the thin coatings with instruments and techniques developed for this purpose. The units are in giga pascals (GPa) due to the extremely high hardness of these coatings. For reference the hardness of diamond is 100 GPa.

Rockwell C hardness indentation is used for a qualitative assessment and relative ranking of the coating adhesion by observing the coating condition around the indentations. Scratch testing procedure developed by CSM Instruments [18] was used to determine the coating adhesion strength.

For the SPE testing, the erodent used was 50 μm alumina and the back pressure of the nozzle was set at 20 psi, as per ASTM Standard G-76-4. A pulsed blast was used to minimize the pressure drop during a long duration of spray. In each test, the pulse was on for 10 s; then off for 10 s. This constituted one spray cycle. A total number of ten spray cycles (100 s total), which constituted one test cycle, were applied before the sample was weighed to measure the weight loss per test cycle. The LDE tests are in progress, and the results will be reported in a future article.

Results and Discussions

Morphological and Microstructural Analysis. Results from a previous study conducted on the surface morphology and cross section of the TiN and TiSiCN coatings were covered in an earlier paper [13]. It was found as the coating thickness increased for the monolayer coatings, the microstructure changed. A thin coating (7 μm) looks very dense and featureless, while for the thicker coatings (25 μm and 43 μm), features of V-shaped columnar internal discontinuities appear. No significant difference in the microstructural quality of the coating was observed between the Ti–6Al–4V and stainless steel substrates. At a lower thickness the surface was smooth, but when the coating was thicker (25 μm and above), the surface was rougher indicating the formation of a crystalline structure with preferred orientation. TiSiCN coating microstructure is a strong function of TMS flow rate as discussed in Ref. [13].

It has been reported that nanocomposite coatings are produced when Si is added to the TiN, and other transition metal nitrides [19]. When the concentration of Si is near 5–10 at. %, the hardness approaches a very high value >40 GPa [19,20]. In this study, a Ti target was sputtered to obtain Ti, while Si, C, and N came from the N_2+TMS environment. To obtain the carbonitrides, an initial N_2 flow was started, which formed stoichiometric nitrides in these TiN coating trials. Then the TMS flow rate was varied. Based on the EDS data, at a TMS flow rate of 3 SCCM (SCCM denotes cubic centimeter per minute at STP), about 10% Si was obtained and this flow rate was then selected to prepare the thick coatings.

Stellite coating evaluation. Stellite coating was deposited onto 17-4PH substrate using the PEMS process. Both monolayer and multilayer recipes were tried under a given ion bombardment ratio to obtain dense coating. The thickness range of these coatings was from 30 μm to 40 μm. For the multilayer coating, the flow of nitrogen was turned on and off for specific time periods. Figure 3 shows the microstructure of these coatings. The coatings appear dense with no internal defects and good surface morphology. However, under the solid particle erosion tests the coating did not perform well. There is little improvement from the stellite coating on the erosion resistance. The coating yielded similar erosion results as the uncoated solid stellite substrate sample. An erosion test sample and test results are shown in Fig. 4 as cumulative mass loss versus the number of test cycles. The erosion rate is linear

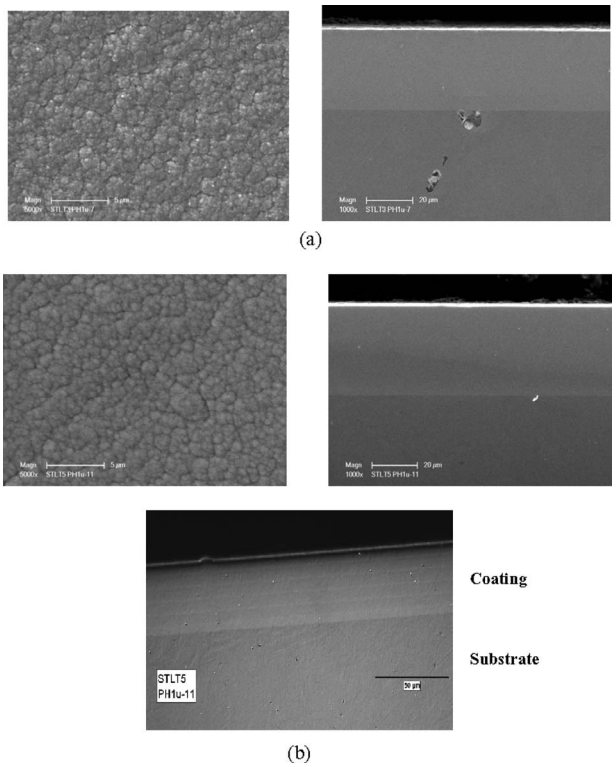

Fig. 3 Topological (left) and cross-sectional (right) images of stellite coating deposited on the 17-4 PH substrate; SEM secondary electron images. (*a*) With no nitrogen (straight stellite) and (*b*) multilayer coating with and without nitrogen (multilayer is visible in the optical microscope photo at bottom).

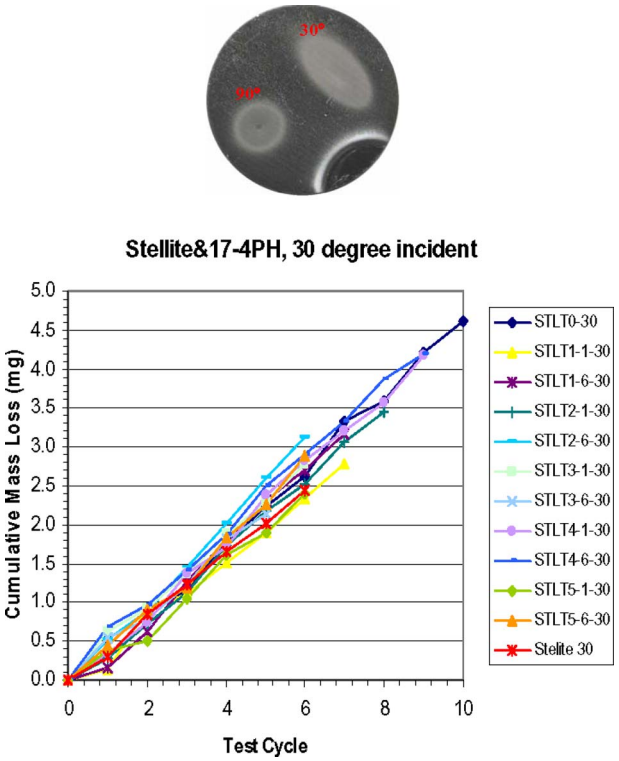

Fig. 4 Example of a coated and tested disk specimen (top) and erosion test results at the 30 deg incident angle. STLT0-30 is the substrate 17-4PH with no coating. Stellite 30 is the sample prepared from the Stellite 6 plate stock. Results from 90 deg tests are similar.

with the number of test cycles; i.e., the weight of sand used and the results from several samples fall in a narrow scatter band. Further study of the stellite coatings was discontinued due to this lack of improvement in the erosion performance.

Ranking of microstructure. The microstructure of the coatings produced using several processing parameters were ranked based on extensive SEM evaluations. They were ranked from a subjective scale of 1–4, 1 being the best. Some examples are shown in Fig. 5. Microstructure ranked 3 (Fig. 5(*a*)) shows columnar growth in the coating and needlelike surface morphology. This condition is undesirable. The other two microstructures are very dense with smoother surfaces. X-ray diffraction analysis for grain size on several samples yielded grain sizes in the range of 5–20 nm.

Nanoindentation tests. Nanoindentation tests were conducted at NRC, Canada. The nanohardness values fall in the range of 20–40 GPa (~1800–4000 HV) for the various coatings in this study. The hardness values of TiSiCN fall within the "super hard" coating regime [20]. It is also noted that the nanocomposite, TiSiCN, has a good combination of high hardness and lower modulus than single-phased TiN. For comparison, the hardness of diamond is 100 GPa on the same scale. Seven measurements were taken on each sample. The nanohardness measurements are repeatable and accurate with low scatter in the data. NRC reported standard deviations ~2–4 GPa (~185–350 HV) for these measurements.

Coating Adhesion Tests. Two methods were used to assess the coating adhesion to the substrate. The first one is a qualitative method by comparative ranking using Rockwell C indentation. The second method is a more quantitative technique where a scratch mark is produced on the coated sample by a diamond stylus under increasing load. The details of these methods and the results are summarized below.

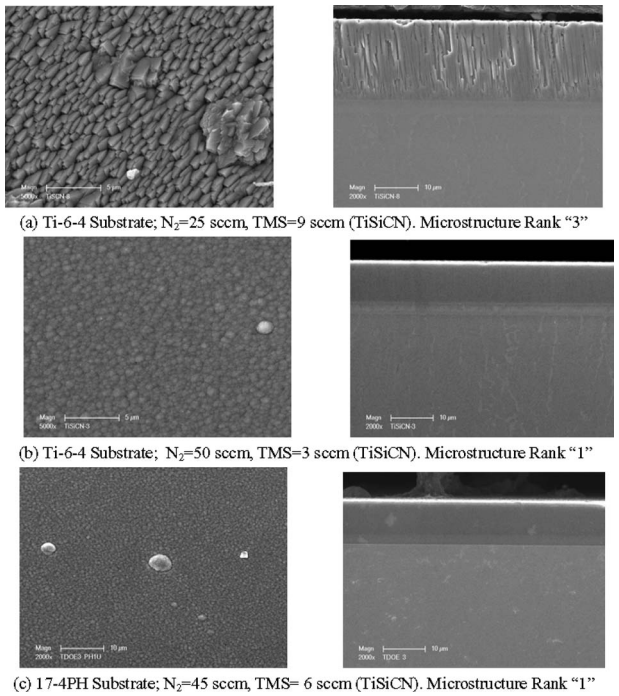

Fig. 5 Microstructural quality of TiSiCN coating on two substrates at different coating deposition process variables. Rank 1 is the best structure.

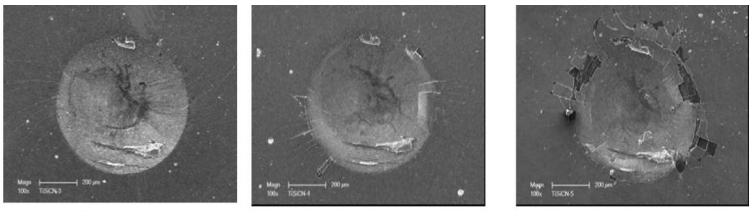

(a) Rank 1 (slight cracking; no delamination) (b) Rank 2 (moderate cracking; some delamination) (c) Rank 3 (severe cracking and spallation)

Fig. 6 Example of coating adhesion strength assessment of TiSiCN nanocomposite coatings on Ti alloy substrate using R_c Hardness indentations. The coating thickness is ~10 μm on these three samples.

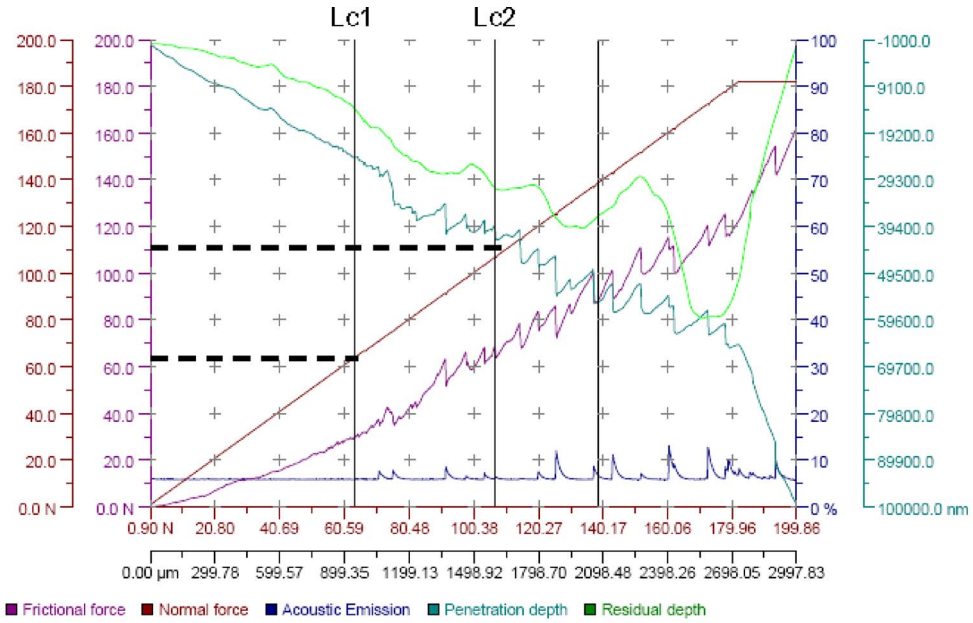

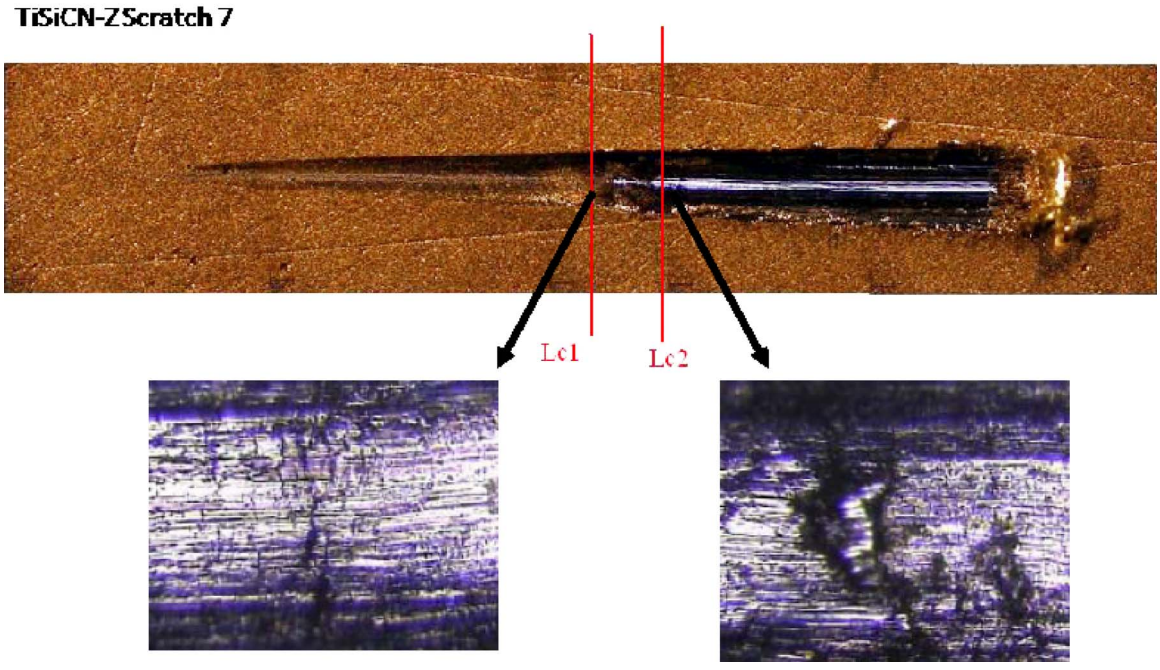

Fig. 7 Example of scratch test data for quantitative measurement of the adhesion strength of the coating on C-450 substrate, monolithic TiSiCN. Top: traces of the various parameters recorded during the scratch test (Sample C3G). Bottom: scratch (about 3 mm long) on a sample coated with TiSiCN nanocomposite. Lc1 (64N) shows the start of coating cracking and at Lc2 (106N) delamination and spallation.

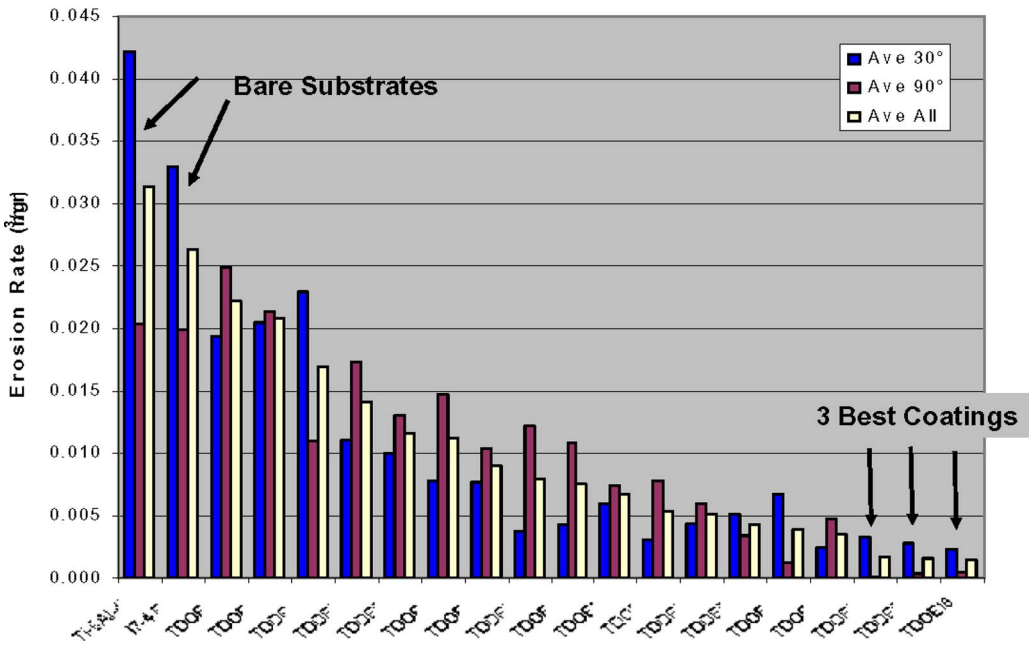

Fig. 8 Solid particle erosion (SPE rate comparison of Ti–6Al–4V and 17-4PH samples coated with TiSiCN coating using various processing parameters. Better coatings are toward the right side of the plot with lower erosion rates. The 3 best coatings are TDOE 12, 13, and 18.

Rockwell C hardness indentation. Conventional Rockwell C (R_c) hardness indentations are used for relative comparison of the coating adhesion to the substrate. The hardness indenter produces a strong localized strain on the coating and the substrate. After the hardness indentation is made the samples are examined under an optical microscope. If the coating has strong adhesion to the substrate, no cracking or spalling will be observed. Otherwise, varying degrees of coating cracking and spallation will be seen around the edges of the indentation mark. Examples of results of such tests on the current samples are shown in Fig. 6. The samples were coated using different coating parameters in the PEMS chamber. They all have similar thicknesses of about 10 μm. Varying degrees of coating spallation can be seen around the rim of the indentation marks of the three indentations. A qualitative ranking is given from 1–3 based on the observed condition of the coating. Rank 1 is the best where no cracking or slight cracking is seen. Moderate cracking and slight delamination is given Rank 2. More severe cracking and coating spallation is given a rank of 3. This ranking in association with the erosion results and microstructural results is used to select the best coating in the series for further evaluation and testing.

Scratch testing. In this second method, a diamond stylus, which is identical to the Rockwell C indenter, is drawn across the coated surface of the coated specimen at a constant speed with progressively increasing normal force. This test method is covered by ASTM Specification C1624-05 [18]. Recorded test variables are (a) normal force, (b) frictional force, (c) acoustic emission signal, (d) penetration depth, and (e) residual depth. The applied variable is the normal force and the speed of the coated sample with respect to the stylus. The damage along the scratch track is microscopically assessed using an optical microscope or SEM as a function of the applied force. An example of a scratch produced in this test on a TiSiCN coated sample and the associated test variables are shown in Fig. 7. Location Lc1 is associated with the start of coating cracking indicating cohesive failure in the coating. Location Lc2 is associated with coating chipping, delamination, and spallation of the coating indicating adhesive failure between the substrate and the coating. In the example shown, the load corresponding to location Lc1 is 64 N and that at Lc2 is 106 N. Initial results from multilayer coating also show that the monolithic and multilayer adhesion strengths fall in the same range for similar coating thicknesses. Results from such results from the various coated samples will be used in conjunction with the R_c indentation results and the erosion test results to develop an overall coating ranking and quality assessment procedure.

Solid particle erosion testing. Alumina sand erosion data for bare Ti–6Al–4V and 17-4PH samples along with TiSiCN coated samples are shown in Fig. 8. Erosion rate (volume loss) results from 30 deg and 90 deg incident angles and the average values of the two are plotted. A density of 4.4 g/cm^3 was used for Ti–6Al–4V, and a density of 7.8 g/cm^3 was used for the stainless steels. The theoretical density of 5.43 g/cm^3 for TiN coating was used to calculate the volume loss of the coated samples. Data from two uncoated substrate alloy samples and 18 other samples coated under various processing conditions are included in this figure. The average values are used only to rank the specimens from left to right in this plot, the right most being the best coating. In general the uncoated ductile substrates and hard coatings have opposite trends at low and high angles of incidence, as illustrated in Fig. 9 [21]. The ductile materials have a better erosion resistance at high angles of incidence, and the brittle materials are better at low angles. This tendency is also observed in the current coatings and substrates. The erosion resistance is affected by the process variables in the PEMS, which produced coatings with different microstructures and thicknesses. The three samples tests by design of experiments (TDOE) 12, 13, and 18 yielded the best erosion resistance. The coating thickness for these three samples is ~20 μm. It should be pointed out that the processing parameters used in this series of tests were optimized from those reported in Ref. [13]. These three samples show improvements by a factor of one to two orders of magnitude (10–100 times) compared to the bare substrates. The erosion rates at 30 deg incidence are higher than that at 90 deg for these three samples, i.e., a tendency toward "ductile" behavior. It may be postulated that the "toughness" of these coatings, which is a combination of hardness

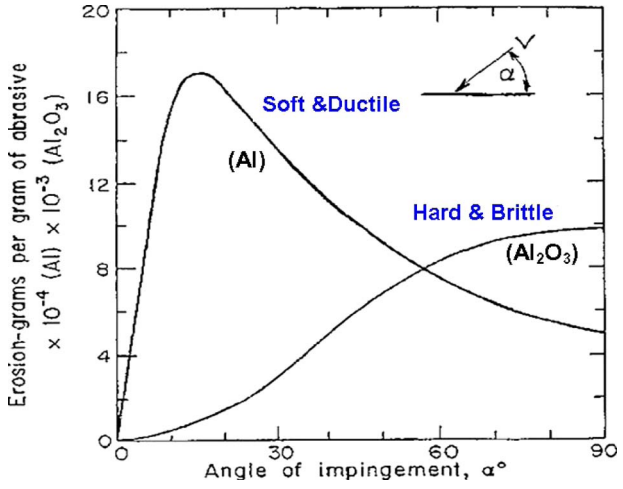

Fig. 9 Erosive mass loss as a function if incident angle for ductile (Al) and brittle (aluminum oxide) materials showing typical "ductile" and "brittle" responses to solid particle erosion. Note the variation in the magnitude of erosion in the *Y* axis label.

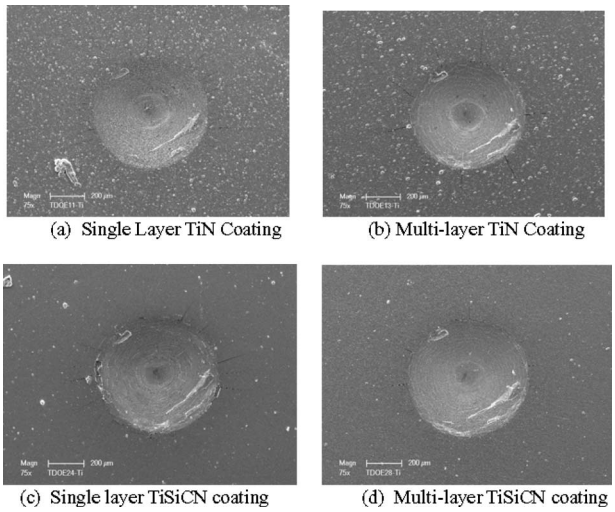

Fig. 12 Rockwell C hardness indentations on four coatings on custom 450 stainless steel substrate showing good adhesion (Rank 1)

and ductility, is better for these three coatings. The grain sizes for these three coatings are 5.6 nm, 6.9 nm, and 7.2 nm, which are at the lower end for the 18 samples studied. The extremely fine grain size could contribute to the increased erosion resistance. Thus, the microstructural features of the PEMS coatings differ significantly from those of the traditional CAPVD coatings. Processing variables corresponding to these three coatings were selected for further development and qualification. LDE tests are in progress on samples prepared using three substrates and three coatings. These results will be published in the future.

Multilayer coatings. Some multilayer coatings were also produced in this project with the Ti–TiN and Ti–TiSiCN combinations. Various coating properties were evaluated similar to those discussed above. Figures 10 and 11 show the typical microstructure of the two multilayer coatings. R_c indentations indicate that they have good adhesion strengths, as shown in Fig. 12. The erosion results are summarized in Fig. 13 as a bar chart. Bare substrates and monolithic coatings deposited to verify the reproducibility of the coating by the PEMS process are also included in this plot for comparison. Even though the multilayer coatings provide significant improvement over the bare substrates especially at 30 deg incidence, they do not seem to provide additional advantage over the single layer coatings at 90 deg incidence. This may be due to the poor erosion resistance of the softer intermediate Ti layers. The thickness and the number of the soft and hard layers may also play a role in the erosion resistance. The fine alumina particle size may also influence the erosion rates. Further testing with varying the layer thicknesses, particle size, and incident angles may shed lighter on this issue.

Figure 14 shows the erosion rate comparison of bare substrates, a commercially produced monolithic TiN coating by a CAPVD process, and two nanocomposite monolithic coatings. These results are in agreement with the previously published results indicating that the TiSiCN outperforms other nitrides against erosion [13,22]. The nanocomposite coatings show significant improvement over the traditional commercial coatings.

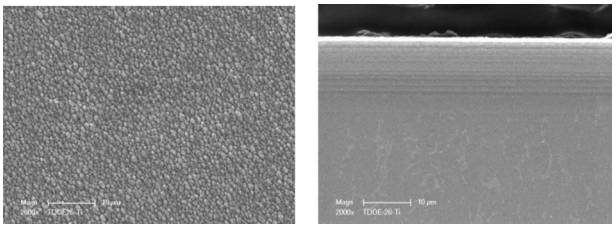

Fig. 10 SEM images of surface morphology (left) and cross section (right) of a multilayered TiSiCN coating

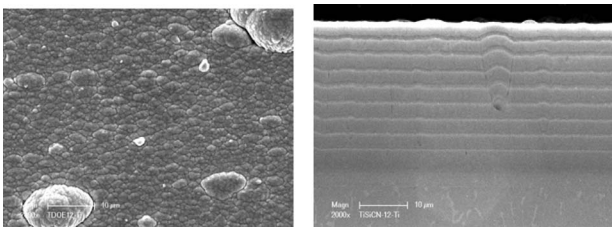

Fig. 11 SEM images of surface morphology (left) and cross section (right) of a multilayered TiN coating

Summary

A plasma enhanced magnetron sputtering method is successful in depositing monolithic TiN, Stellite 6, and nanocomposite Ti-

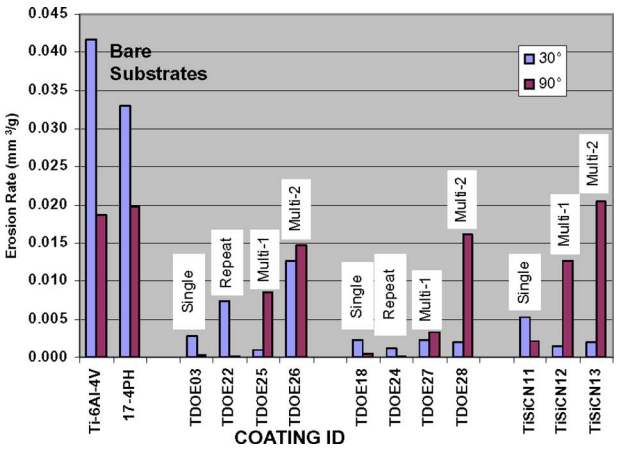

Fig. 13 Solid particle erosion test results on single and multilayer coatings produced under different processing conditions showing significant erosion resistance. Single layer coatings are better than the multilayer coatings under SPE.

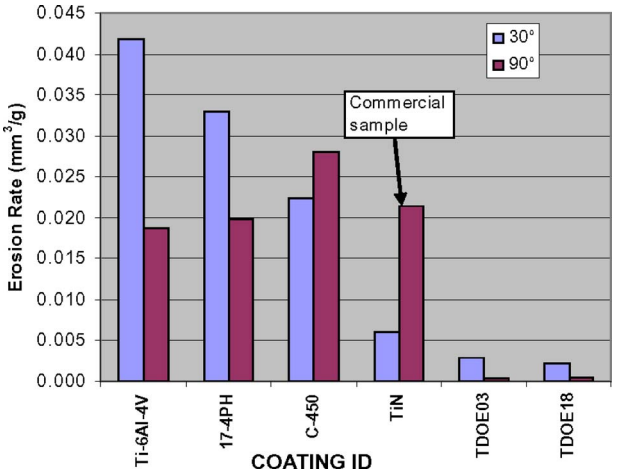

Fig. 14 Comparison of erosion rates of commercial TiN coating by CAPVD and the advanced nano-composite coatings by PEMS

SiCN coatings; and multilayer coatings on Ti–6Al–4V and stainless steel substrates. Thickness of the coatings ranged from 10 μm to 40 μm. Coatings have been deposited using several combinations of process variables to identify the optimum process to obtain the best combination of physical and mechanical properties. The selection of TMS gas to produce the nanocomposite coating as the precursor for Si is a novel approach, which allows one to deposit nanocomposite coatings without much difficulty compared to the use of other complex target materials and gasses. Microstructure, hardness, adhesion strength, and erosion resistance were used to rank the coatings in their performance. Processing variables have significant effect on these properties. PEMS processed Stellite 6 coating did not show much improvement in the erosion resistance over the bare substrates. Specific set of processing variables have been identified to produce the best TiN and fine grained TiSiCN nanocomposite coatings by the PEMS process. Reproducibility of the coatings by the PEMS has been verified for some of the selected coatings in repeat deposition tests. These coatings outperform the monolithic TiN nitride coatings and show erosion resistance improvement of over an order of magnitude. Deposition of single and multilayer coatings was carried out. Initial SPE tests show that the multilayer coating may not have added advantage at high angles of incidence compared to monolithic coatings. Mechanical test specimens have been coated to evaluate the effects of the selected coatings on tensile and high-cycle fatigue properties of the three alloys. Liquid droplet erosion tests are also in progress on coated samples.

Acknowledgment

This work was supported by EPRI, and some of the results were generated under a SwRI internal research project. The authors wish to thank Edward Langa for assistance in preparing the coated samples and conducting the solid particle erosion tests. Byron Chapa and Christopher Wolfe assisted with the metallurgical laboratory work. Dr. Qi of NRC Canada is thanked for the nanohardness tests. CSM Instruments Inc. conducted the scratch tests.

References

[1] Tabakoff, W., 1989, "Investigation of Coatings at High Temperature for Use in Turbomachinery," Surf. Coat. Technol., **39/40**, pp. 97–115.
[2] DeMasi-Marcin, J. Y., and Gutpa, D. K., 1994, "Protective Coatings in the Gas Turbine Engine," Surf. Coat. Technol., **68/69**, pp. 1–9.
[3] Electric Power Research Institute, 1999, *Turbine Steam Path Damage: Theory and Practice, Vol. 2: Damage Mechanisms*, Electric Power Research Institute, Palo Alto, CA.
[4] Swaminathan, V. P., 2004, "Investigation of High-Pressure Compressor Blade Failures in LM6000 Sprint Engines," Western Turbine Users and Combustion Turbine Operators Task Force Conferences, Mar.
[5] Rickerby, D. S., and Burnett, P. J., 1987, "The Wear and Erosion Resistance of Hard PVD Coatings," Surf. Coat. Technol., **33**, pp. 191–211.
[6] Veprek, S., 1998, "New Development in Superhard Coatings: The Superhard Nanocrystalline-Amorphous Composite," Thin Solid Films, **317**, pp. 449–454.
[7] Diserens, M., Patscheider, J., and Levy, F., 1998, "Improving the Properties of Titanium Nitride by Incorporation of Silicon," Surf. Coat. Technol., **108–109**, pp. 241–246.
[8] Musil, J., 2000, "Hard and Superhard Nanocomposite Coatings," Surf. Coat. Technol., **125**, pp. 322–330.
[9] Rebouta, L., Tavares, C. J., Aimo, R., Wang, Z., Pischow, K., Elves, E., Rojas, T. C., and Odriozola, J. A., 2000, "Hard Nanocomposite Ti–Si–N Coatings Prepared by DC Reactive Magnetron Sputtering," Surf. Coat. Technol., **133–134**, pp. 234–239.
[10] Matossian, J. N., Wei, R., Vajo, J., Hunt, G., Gardos, M., Chambers, G., Soucy, L., Oliver, D., Jay, L., Tylor, C. M., Alderson, G., Komanduri, R., and Perry, A., 1998, "Plasma-Enhanced, Magnetron-Sputtered Deposition (PMD) of Materials," Surf. Coat. Technol., **108–109**, pp. 496–506.
[11] Wei, R., Vajo, J. J., Matossian, J. N., and Gardos, M. N., 2002, "Aspects of Plasma-Enhanced Magnetron-Sputtered Deposition (PMD) of Hard Coatings on Cutting Tools," Surf. Coat. Technol., **158–159**, pp. 465–472.
[12] Fortuna, S. V., Sharkeev, Y. P., Perry, A. P., Matossian, J. N., Shuleopov, A., 2000, "Microstructural Features of Wear Resistant Titanium Nitride Coatings Deposited by Different Methods," Thin Solid Films, **377–378**, pp. 512–517.
[13] Swaminathan, V. P., Wei., R., and Gandy, D. W., 2007, "Erosion Resistant Nano Technology Coatings for Gas Turbine Components," ASME Paper No. GT2007-27027.
[14] Huo, D.-H., and Huang, K.-W., 2001, "A New Class of Ti–Si–C–N Coatings Obtained by Chemical Vapor Deposition—Part I: 1000°C Process," Thin Solid Films, **394**(1-2), pp. 71–79.
[15] Huo, D.-H., and Huang, K.-W., 2001, "A New Class of Ti–Si–C–N Coatings Obtained by Chemical Vapor Deposition—Part II: Low-Temperature Process," Thin Solid Films, **394**(1-2), pp. 80–88.
[16] Huo, D.-H., and Huang, K.-W., 2002, "A New Class of Ti–Si–C–N Coatings Obtained by Chemical Vapor Deposition—Part III: 650–800°C Process," Thin Solid Films, **419**(1-2), pp. 11–17.
[17] Ma, D., Ma, S., Dong, H., Xu, K., and Bell, T., 2006, "Microstructure and Tribological Behavior of Super-Hard Ti–Si–C–N Nanocomposite Coatings Deposited by Plasma Enhanced Chemical Vapor Deposition," Thin Solid Films, **494**, pp. 438–444.
[18] ASTM Specification: C 1624-05, 2005, "Standard Test Method for Adhesion Strength and Mechanical Failure Modes of Ceramic Coatings by Quantitative Single Point Scratch Testing," ASTM International, West Conshohocken, PA.
[19] Veprek, S., Nesladek, P., Niederhofer, A., Glatz, F., Jilek, M., and Sima, M., 1998, "Recent Progress in Superhard Nanocrystalline Composites: Towards Their Industrialization and Understanding of Origin of the Superhardness," Surf. Coat. Technol., **108–109**, pp. 138–147.
[20] Hauert, R., and Patscheider, J., 2000, "From Alloying to Nanocomposites—Improved Performance of Hard Coatings," Adv. Eng. Mater., **2**(5), pp. 247–259.
[21] Finnie, I., 1994, "Some Reflections on the Past and Future of Erosion," *Proceedings of the 8th International Conference On Erosion by Liquid and Solid Impact*, I. M. Hutchings and J. A. Little, eds., Cambridge, UK, Sept. 4–8.
[22] Wei, R., Langa, E., Rincon, C., and Arps, J., 2006, "Solid Particle Erosion Protection of Turbine Blades With Thick Nitrides and Carbonitride Coatings From Magnetron Sputter Deposition," *Proceedings of ASM International Surface Engineering Conference (ISEC)*, Seattle, WA, May.